t. Space Sci., Vol. 40, No. 12, pp. 1585–1597, 1992
ed in Great Britain.

0032-0633/92 $5.00+0.00
Pergamon Press Ltd

RADIATIVE CONSTRAINTS ON THE ENERGY BUDGET OF THE TROPICAL ATMOSPHERE

K. MINSCHWANER* and M. B. McELROY
Department of Earth and Planetary Sciences and Division of Applied Sciences,
Harvard University, Cambridge, MA 01238, U.S.A.

Abstract—A simple one-dimensional model is presented to describe the energy budget of the tropical atmosphere. Heating of the atmosphere is associated primarily with latent energy released due to precipitation in localized regions of intense cumulonimbus activity. Air transported to upper regions of the troposphere by cumulonimbus systems is returned to the surface over a large region of descent. Heat released by subsidence is balanced primarily by emission of radiation in the infrared. The model accounts for this energy balance, exploring specifically the constraints on permissible fluxes of mass and energy.

Results suggest that the strength of the background subsidence field in the tropics may be sensitive to surface temperature and to changes in atmospheric composition, specifically variations in the altitude distribution of H_2O and changes in the abundance of greenhouse gases such as CO_2. The mean level of detrainment of deep cumulonimbus clouds is found to increase with increasing surface temperature. This behavior is shown to be sensitive to atmospheric composition. The surface temperature for an atmosphere containing twice the present level of CO_2 is predicted to increase by 1.4K, about 25% less than the change obtained with models in which the lapse rate of temperature is specified at lower altitudes, where assumptions of radiative equilibrium would lead otherwise to a statically unstable condition.

Buoyancy considerations suggest that there may be an upper limit to the range of permissible values for surface temperature in the tropics. Models in which the subsidence mass flux is assumed constant with respect to altitude are found to be unable to maintain buoyancy for rising air in the face of heat released by descent when surface temperatures exceed about 312K.

1. INTRODUCTION

The mean thermodynamic state of the atmosphere in the maritime tropics is determined by interactions involving a number of physical processes: radiative cooling by infrared (i.r.) emission, transport of heat and moisture (both by cumulus clouds and by the large-scale flow) and turbulent transfer of sensible and latent heat from the surface to the atmosphere. A simplified division of the tropical atmosphere into four regions, as indicated in Fig. 1, provides a useful illustration of these processes. Region 1 is distinguished by deep cumulonimbus towers which extend to the tropopause, penetrating, in some cases, to the lower stratosphere. A large fraction of the moisture condensed in the deep clouds falls out as precipitation. The resultant latent heating, however, is not immediately imparted to the local environment; instead this heat is used mainly to increase the sum of internal and potential energies of cloud air parcels. The heat is realized in cloud-free areas of region 1 and over a large, generally cloud-free, area of descent, region 2.

Subsidence of air in region 2 results in heating by compression. It is important to realize that subsidence also occurs over a large part of region 1 since the fraction of this area occupied by deep clouds is small. Subsidence heating in both regions is balanced by radiative cooling associated with emission of i.r. radiation to space. The moisture content of the subsiding air is exceedingly low; the relative humidity is rarely above 50%, usually averaging about 20%–30% (Newell *et al.*, 1972). Air leaves region 2 and enters

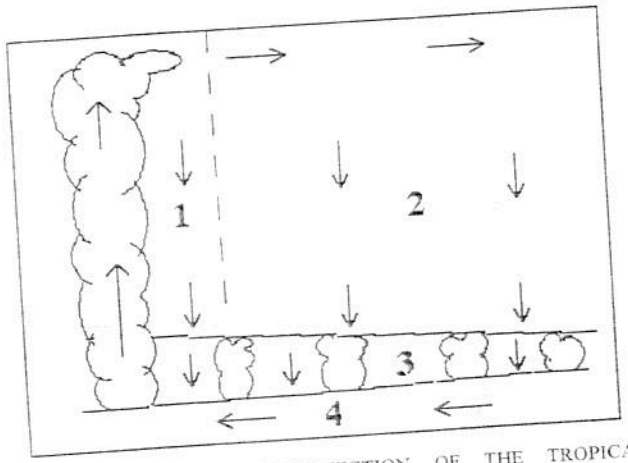

FIG. 1. SCHEMATIC CROSS-SECTION OF THE TROPICAL ATMOSPHERE.

The figure shows a simplified diagram for the mean circulation and structure of the tropical atmosphere. Region 1 contains deep cumulonimbus clouds which pump warm, moist air from the surface to the tropopause. Region 2 is characterized by gentle subsidence. Region 3 contains small, non-precipitating cumulus clouds, capped by a strong inversion. The flow in region 4 is back towards region 1.

* Present address: National Center for Atmospheric Research, P.O. Box 3000, Boulder, CO 80307, U.S.A.

region 3, the trade cumulus layer, after crossing through the trade inversion. The inversion is characterized by an abrupt change in the fields of moisture and temperature, typically at an altitude between about 1 and 3 km. The trade cumulus layer is dotted with shallow, non-precipitating cumulus clouds. These clouds do not impart heat to the layer. Rather, they act to moisten it through transference of water from region 4.

Air subsiding between the trade cumuli eventually reaches the mixed layer, region 4, located between the base of the cumulus clouds and the surface. Traveling back to region 1 within the mixed layer, air parcels pick up heat and moisture from the sea surface. There is a gradient in sea surface temperature (SST) of between 3 and 5K over region 4, with the warmest water typically below region 1. For the present climate, deep clouds generally appear over warm pools where SSTs range from 300 to 302K. In contrast, horizontal gradients in temperature above the trade wind inversion are small; the Coriolis effect is simply too weak at low latitudes to support large horizontal gradients of pressure within the free troposphere.

The pattern in Fig. 1 defines a closed circuit: air parcels ascending in cumulonimbus towers conserve their initial moist static energy; the static energy decreases as a result of radiative cooling during clear-air descent; the moist static energy of air increases in the trade cumulus layer due to addition of moisture; the parcel recovers its initial value of moist static energy in the mixed layer, drawing on moisture and sensible heat from the sea surface. Figure 1 could be regarded as a crude meridional cross-section of the Hadley regime, with region 1 corresponding to the intertropical convergence zone (ITCZ) and region 2 representing the subtropical high. This description could apply equally well to the Walker circulation, in which case regions 1 and 2 would be associated with the domains of the Western and Eastern Pacific, respectively.

At any given time, less than 1% of the total area of the tropics is occupied by deep cumulonimbus clouds (Riehl and Malkus, 1958). A large fraction of the tropical atmosphere is characterized by subsidence in the free troposphere above regions 3 and 4. We focus in this paper on regions 1 and 2, inferring changes for the circuit as a whole by examining the behavior of key quantities such as the subsidence mass flux, the latent heat flux at the surface and the emergent flux of i.r. radiation at the top of the atmosphere in a series of one-dimensional steady-state calculations. Section 2 describes the physical basis of the model and develops the methodology used to obtain the results presented in Section 3. The response of the model to changes in surface temperature, relative humidity and CO_2 are discussed in Section 3. The subsidence mass flux is shown to decrease with increasing surface temperature. Results indicate that a model characterized by a constant, height-independent, subsidence mass flux implies a maximum value for the amount of solar energy that can be absorbed by the surface–atmosphere system. Concluding remarks are presented in Section 4.

2. MODEL DESCRIPTION

The formalism of the model employed here was outlined first by Schneider (1977) and Sarachik (1978). The model explicitly considers the heating of the clear-sky atmosphere associated with deep cumulus convection. It neglects export of energy from the tropics to higher latitudes, a contribution to the energy budget that is small compared to the magnitude of other terms in the energy balance described below. Averaged over the latitude band 0–20°N, this export corresponds to an annual mean cooling of the atmospheric column of about 25 W m^{-2} (Oort, 1971). By way of comparison, the typical magnitude of the rate of i.r. cooling, integrated over a vertical column of atmosphere, is about 140–165 W m^{-2} (Minschwaner and McElroy, 1992).

As discussed previously, saturated air is assumed to rise in cumulus towers (region 1, Fig. 1). The subsidence mass flux, M_c, results from detrainment of mass at the tops of cumulus towers. The return flow acts to heat the clear-sky environment if the atmosphere is statically stable (regions 1 and 2). The clear-sky energy balance is given by:

$$Q_R + c_p M_c \left(\frac{dT}{dz} + \Gamma \right) = 0, \quad z_B \leqslant z \leqslant z_T, \tag{1a}$$

$$Q_R = 0, \quad z > z_T, \tag{1b}$$

where c_p is the heat capacity of dry air, T is temperature, z is altitude, $\Gamma = g/c_p$ is the dry adiabatic lapse rate and Q_R is the radiative cooling rate, given by:

$$Q_R = -\frac{\partial}{\partial z}(F_{IR} - F_S), \tag{2}$$

where F_{IR} is the net upward flux of infrared radiation and F_S is the net downward flux of solar energy. The energy balance indicated by equation (1a) is applied within the troposphere above the top of the mixed layer, z_B, to a height, z_T, defined by the mean level at which clouds are assumed to detrain. The atmosphere

is assumed to be in radiative equilibrium above z_T [equation (1b)].

The subsidence mass flux, M_c, is taken as constant from z_B to z_T. Physically, this corresponds to a situation where entrainment and detrainment by deep cumulonimbus clouds are negligible between z_B and z_T. Deep clouds are assumed to detrain at a common level, z_T. Studies of the large-scale heat and moisture balance in the tropics indicate that the mass flux is approximately constant between about 800 and 300 mb (Yanai *et al.*, 1973; Gray, 1973). Ogura and Cho (1973) found that the mass flux distribution in tropical cumuli is bi-modal, dominated by shallow clouds detraining below 600 mb and by deep clouds penetrating to levels above 300 mb. The mean downward velocity in the clear-sky tropics has been measured by Doppler radar techniques (Balsley *et al.*, 1988). The results are reproduced in Fig. 2, where the vertical velocity has been converted to mass flux by adopting a density profile according to the reference tropical atmosphere given by McClatchey *et al.* (1972). The mass flux profile consistent with equation (1) is also shown in Fig. 2, calculated based on the temperature structure and radiative cooling rates from the reference tropical atmosphere. It is not clear why the calculated mass flux is significantly less than the observed flux between 6 and 11 km. For comparison, it will be demonstrated that a satisfactory simulation of the present tropical atmosphere can be achieved by assuming a constant mass flux of about 3×10^{-4} g cm^{-2} s^{-1} between 1 and 13 km.

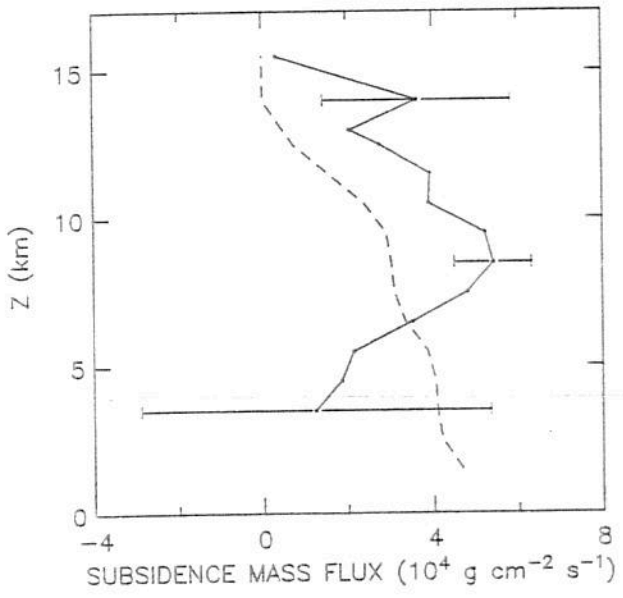

FIG. 2. CLEAR-SKY PROFILES OF SUBSIDENCE.
The solid curve represents the observed mean subsidence during undisturbed conditions over the Western tropical Pacific (Balsley *et al.*, 1988). Horizontal bars indicate reported uncertainties in the measurements. The dashed curve indicates rates required to balance the rate of radiative cooling, based on the reference tropical atmosphere given by McClatchey *et al.* (1972).

Equations (1a) and (1b) require an independent boundary condition; solutions can be implemented by specifying, for example, the magnitude of F_S at the top of the atmosphere, or a value for the temperature at z_B. Once the boundary condition is chosen, it is possible, in principle, to obtain a solution for specified values of the parameters z_B, z_T and M_c. There is no assurance, however, that the solution obtained in this fashion will be consistent with the physics of the real atmosphere. As in many idealized models of complicated physical systems, the method of closure represents one of the most critical aspects of the problem. We need a consistent, physically-based procedure to link z_B, z_T and M_c to the dependent variables in the problem, specifically the variation of temperature with altitude.

We assume that turbulent mixing below z_B is sufficient to homogenize quantities such as potential temperature and the mixing ratio of water vapor in the mixed layer, so that z_B can be identified with the mean altitude of the cloud base. For specified conditions of temperature and relative humidity at the surface, z_B and $T(z_B)$ can be determined by calculating the lifting condensation level using, for example, expressions presented by Bolton (1980). Furthermore, to a good approximation, ascent of air within deep cumulonimbus clouds conserves moist static energy, h. Clouds detrain at z_T when the temperature in the cloud is the same as that for the surrounding environment:

$$h = c_p T + gz + Lq = \text{constant}, \tag{3}$$

which implies:

$$c_p T(0) + Lq(0) = c_p T(z_T) + gz_T. \tag{4}$$

Here L is the latent heat of condensation of water and q is the mixing ratio of water vapor. The left-hand side of equation (4) represents the initial moist static energy of cloud parcels. The right-hand side defines the static energy of the clear-sky environment at z_T; we neglected here the contribution from latent energy, since the magnitude of this term typically is less than 1% of the total static energy at altitudes greater than 10 km.

It is important to point out the consequences of the seemingly innocuous assumptions contained in equation (4). The connection between the surface and z_T through the deep clouds implies that the model boundary condition corresponds to the state of the mixed layer in the warm pool region. The clear-air temperatures represent a much larger tropical

domain, but it should be emphasized that the solution is always linked, through equation (4), to the thermodynamic properties of surface air over the warm pool.

According to this simple model of the tropical atmosphere, net radiative cooling of the atmospheric column is related to the flux of latent heat arising from the surface, as indicated by the integral energy budget:

$$-\int_{z_B}^{z_T} Q_R \, dz = c_p M_c \int_{z_B}^{z_T} (dT/dz + \Gamma) \, dz$$

$$F_N(z_T) - F_N(z_B) = M_c \{c_p[T(z_T) - T(z_B)] + gz_T - gz_B\}, \quad (5)$$

where $F_N = F_{IR} - F_S$ is the net radiative flux.

Net radiative cooling in the mixed layer is balanced by the flux of sensible heat from the surface, Q_S:

$$F_N(z_B) - F_N(0) = Q_S. \quad (6)$$

In addition, the assumption that potential temperature is constant in the mixed layer implies that:

$$c_p T(0) = c_p T(z_B) + gz_B. \quad (7)$$

Combining equations (4), (5) and (7) gives:

$$F_N(z_T) - F_N(z_B) = M_c L q(0). \quad (8)$$

Heating at the surface associated with the net downward flux of radiation is balanced by cooling induced by the upward flux of latent and sensible heat:

$$F_N(0) + LE + Q_S = 0, \quad (9)$$

where E represents the rate of evaporation from the sea surface. The emergent flux of i.r. radiation at the top of the atmosphere must balance the absorbed solar energy: $F_N = 0$. Since the atmosphere above z_T is in radiative equilibrium [equation (1b)], it follows that $F_N(z_T) = 0$. Substituting equations (6) and (9) into equation (8), we obtain:

$$LE = M_c L q(0). \quad (10)$$

Equation (10) ensures that the flux of water vapor into precipitating cumulus clouds is replaced by the evaporative flux from the surface.

It is worthwhile to summarize the conceptual outline of the model to this point. Net absorption of radiation at the sea surface is balanced by evaporative cooling and by turbulent transfer of sensible heat to the atmosphere [equation (9)]. Sensible heat is deposited within the mixed layer, below z_B [equation (6)]. Latent heat is transported upward to z_T within the cores of deep cumulonimbus towers [equation (4)]. The associated heat is deposited in the free troposphere between z_B and z_T as the air subsides, with rates of radiative cooling [equation (1a)]. Net radiative cooling of the troposphere between z_B and z_T is determined by the supply of latent heat contributed by evaporation at the surface [equations (8) and (10)]. The levels z_B and z_T are related according to the thermodynamic properties of air in the mixed layer over the warm pool region. The parameter M_c is the most critical unknown that remains to be determined.

One way to specify M_c is to employ aerodynamic formulae to parameterize the rate of evaporation at the surface (Lindzen *et al.*, 1982; Sun and Lindzen, 1992):

$$E = C_D U_* [q^*(T_s) - qT(0)]. \quad (11)$$

Here, T_s is the surface temperature and $T(0)$ is the air temperature at the ground; q^* refers to the saturation mixing ratio of water vapor; C_D is an aerodynamic drag coefficient and U_* is an appropriate measure of the horizontal velocity. The mass flux is then determined by equation (10). One drawback to this approach is that the parameters C_D and U_* must be specified. In some sense we have replaced one parameter, M_c, by the product of two, $C_D U_*$. If the temperature discontinuity at the surface is not calculated explicitly by allowing for this jump in the radiative code, we must specify in addition the magnitude of the temperature discontinuity. Satisfactory simulation of the present climate can be obtained by tuning the evaporative flux so that model temperatures are roughly consistent with observations. However, this formulation is unlikely to provide a physically consistent solution to the problem if the boundary conditions, surface temperature for example, are extended beyond the range currently observed.

Figure 3 shows the result of two calculations in which the evaporative flux is parameterized according to equation (11), with the temperature discontinuity at the surface set equal to 1K with the surface relative humidity fixed at 80%. The parameters C_D and U_* were adjusted so that the calculated profile of temperature is consistent with observations for a surface temperature of 299K, as indicated by curve A. Applying the same parameterization to the case in which the surface temperature is 306K leads to the result summarized by curve B. Profiles of temperature within the deep clouds, calculated according to a moist adiabat from z_B to z_T, are indicated by the dotted curves. The moist adiabatic lapse rate was calculated assuming pseudoadiabatic ascent of surface air (Hess, 1959). The problem that arises is that the clear-air temperatures for the case represented by profile B are warmer than temperatures at corresponding levels in the deep clouds (see also Lindzen *et al.*, 1982, Fig.

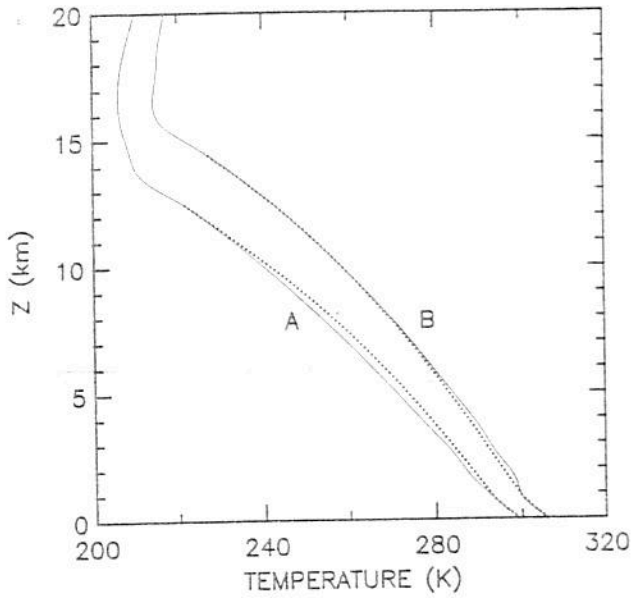

FIG. 3. TEMPERATURE PROFILES FOR $T_s = 299$ AND 306K. The solid curves denote clear-air temperatures calculated by the model; the dotted curves represent cloud temperatures calculated according to the moist adiabat. Profile A was computed using a surface temperature of 299K with a mass flux of 2.9×10^{-4} g cm^{-2} s^{-1}. Profile B was computed for a surface temperature of 306K with a nearly identical mass flux, consistent with the aerodynamic formula for evaporation and a constant value for the temperature discontinuity at the sea–air interface.

cloud parcels, we must require temperatures in the clear-air environment to be cooler than temperatures for air ascending on a moist adiabat originating at the cloud base. The recent study by Satoh and Hayashi (1992) reached similar conclusions involving constraints on the clear-sky thermal structure for this model.

The requirement for positive buoyancy of cloud parcels constrains the range of possible values for M_c. The buoyancy constraint places an upper limit on the magnitude of M_c: if the mass flux exceeds this limit for a given choice of the boundary conditions, then the model produces a solution that is no longer consistent physically with the simple picture in Fig. 1. The problem relates to the net radiative cooling of the troposphere for specified conditions of temperature and composition. For the case where the clear-air profile of temperature is exactly equal to the moist adiabatic limit, the net radiative cooling from z_B to z_T determines the value of the surface evaporation rate, which is related in turn to M_c by the moisture content of surface air [equation (10)]. This determines the maximum value of M_c. Choosing a value for M_c above this limit requires that heat supplied by evaporation at the surface should exceed the net rate of radiative cooling for a moist adiabatic troposphere. The model responds to the dilemma by requiring warmer temperatures in the lower troposphere in order to allow for an increase in the net rate of radiative cooling.

In practice, we expect differences in temperature between the cloud and clear-sky environments to be relatively small. Models of cumulonimbus convection suggest that the temperature difference is unlikely to exceed 5K, with 2–3K appropriate for the maximum updraft velocities observed in cumulonimbus clouds during GATE (Ferrier and Houze, 1989; Lemone and Zipser, 1980). The constraint on the clear-sky temperature structure inferred here for region 1 applies equally well to region 2; as discussed earlier, horizontal pressure and temperature gradients within region 2 and between regions 1 and 2 must be small. The buoyancy constraint may be expressed quantitatively by referring to the convective available potential energy (CAPE) of the clear-sky environment:

$$\mathrm{CAPE} = \int_0^{z_T} g \frac{T_{vc}(z) - T_{ve}(z)}{T_{ve}(z)} \mathrm{d}z, \qquad (12)$$

where T_{vc} is the virtual temperature inside the cloud and T_{ve} is the calculated temperature of the clear-sky environment. Virtual temperature, accounting for the difference in density due to changes in water vapor, is used to assess the buoyancy of air parcels:

$$T_v = T \frac{1 + q/\varepsilon}{1 + q}, \qquad (13)$$

where $\varepsilon = 0.622$ is the ratio of the molecular weight of water to the mean molecular weight of dry air.

Consistent with observation (Xu and Emanuel, 1989), we seek a solution in which the quantity of CAPE in the clear-sky atmosphere is minimized, under the condition that $T_{vc} - T_{ve} \geqslant 0$ at all altitudes. In the following section, we discuss situations where the model has difficulty meeting this criterion.

3. RESULTS

Details of the procedure used to evaluate radiative cooling are described by Minschwaner and McElroy (1992). The model employs the correlated-k method to perform integrations over spectral intervals small enough that the Planck function can be replaced by an appropriate average. Longwave cooling due to water vapor, carbon dioxide and ozone is considered, together with shortwave heating by ozone and water vapor. The finite difference approximation employed to evaluate the vertical flux integral uses a higher order quadrature scheme for optically thick layers to provide a better account of the vertical profile for

radiative cooling. For models imposing a convective adjustment, fixing tropospheric lapse rates to specified values, the specific choice of method for vertical integration is relatively unimportant since the integrated value of the tropospheric cooling rate is well approximated using the mean layer temperature approach (Minschwaner and McElroy, 1992). However, for the model described here the details of the profile of radiative cooling are critical.

A series of calculations was implemented with different values for surface temperature. To examine the sensitivity of the model to changes in the abundance of CO_2, we focused on three scenarios; a CO_2 mixing ratio of 280 ppm corresponding to the preindustrial atmosphere, 350 ppm representing the present atmosphere and 700 ppm simulating a possible condition in the future. Mixing ratios of water vapor in the troposphere were constrained using the fixed profile for relative humidity presented by Manabe and Wetherald (1967). Vertical profiles assumed for water vapor are not strictly consistent with the assumption of a constant, height-independent, subsidence mass flux. The observed distribution of water vapor in the middle and upper troposphere implies detrainment and subsequent evaporation of condensed water from cumulus clouds. We are interested here in applying the simple model, with reasonable assumptions concerning the distribution of water vapor, to study the sensitivity of the mean state of the tropical atmosphere to changes in model parameters. The important point is that the model is successful in capturing the basic features of the contemporary energy balance for the tropics. In the Manabe and Wetherald (1967) formulation, the vertical profile of relative humidity is specified exclusively by the relative humidity at the surface. To assess the sensitivity of the model to changes in water vapor, three cases were considered, corresponding to relative humidities at the surface of 70%, 80% and 90%. The vertical distribution of O_3 was fixed according to the mean profile observed at a latitude of 10 N (Keating and Young, 1985).

Since surface air is undersaturated with respect to H_2O, we calculated the lifting condensation level (z_B) for each value of surface temperature, T_s and imposed a convective adjustment from the surface to this level. The lapse rate in the convective boundary layer was fixed equal to the dry adiabatic value. The temperature at the lifting condensation level was determined by the temperature and relative humidity at the surface, according to the empirical relation derived by Bolton (1980). The energy balance between z_B and z_T, represented by equation (1a), was used to model temperatures for the clear-sky environment; profiles of temperature were calculated using the maximum mass flux consistent with the buoyancy constraint discussed above.

The flux of solar energy absorbed by the atmosphere–surface system was defined by the magnitude of the emergent flux of i.r. radiation at the top of the atmosphere. In a similar fashion, the flux of latent heat from the surface was obtained from the difference in the net radiative flux between z_T and z_B, while the flux of sensible heat at the surface was calculated based on the difference in the net radiative flux between z_B and the surface.

3.1. *Dependence of* M_c *on surface temperature*

The dependence of M_c on surface temperature is illustrated in Fig. 4. In all cases the calculated mass flux decreased with increasing surface temperature. This may seem at odds with the notion that a rise in surface temperature should lead to an increase in cumulus convection, but in the context of our model the result is easily understood. In order to satisfy the buoyancy constraint, we found that the height of the detrainment level was required to increase with increasing temperature; warmer surface temperatures corresponded to higher mean levels for the cloud tops. The value of the parameter z_T ranged from 13 km for $T_s = 299.2$K, to 17 km for $T_s = 311.3$K. A simplified analysis suggests that the height integrated rate of radiative cooling, represented by the left-hand side of

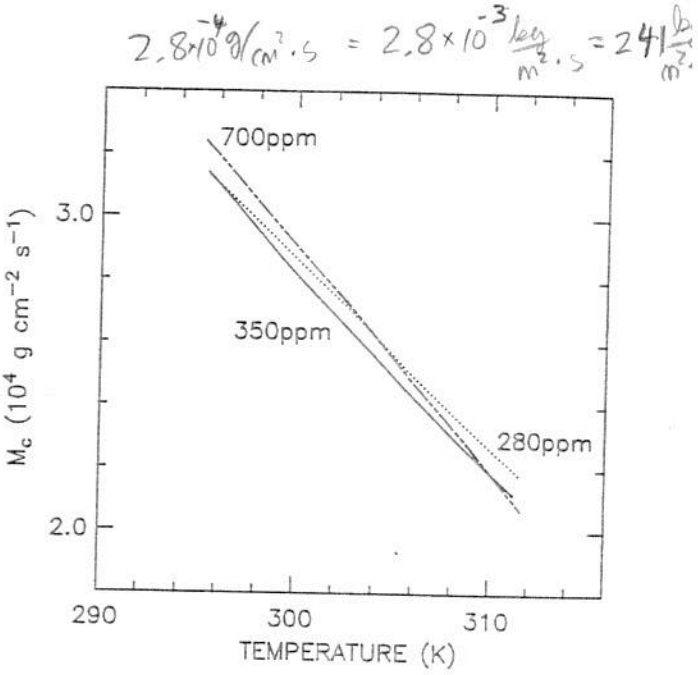

FIG. 4. CUMULUS MASS FLUX VS SURFACE TEMPERATURE. Computed values for the mass flux for a range of surface temperatures corresponding to 280 ppm CO_2 (·····), 350 ppm CO_2 (——) and 700 ppm CO_2 (– · · –) are shown. In all three cases, M_c is observed to decrease with increasing temperature.

equation (5), increases approximately as a fourth order polynomial function of surface temperature. This behavior is apparent in the dependence of the latent heat flux, LE, on surface temperature as shown in Fig. 5. On the other hand, the magnitude of the water vapor mixing ratio at the surface increases exponentially with surface temperature according to the Clausius Clapeyron relationship [as indicated by the curve $Lq(0)$ in Fig. 5]. Since the mass flux is determined by the ratio of the latent heat flux to the mixing ratio for surface water vapor [equation (10)], warmer surface temperatures must be accompanied by a decrease in the magnitude of M_c.

There is a more subtle way to interpret the behavior of M_c with increasing T_s, involving a consideration of temperature lapse rates in the region of the atmosphere immediately below z_T. Recall that the temperature in the region of subsidence must be cooler than the temperature within the zone of cumulus updraft which, it is assumed, is characterized by a moist adiabat from z_B to z_T. The moist adiabatic lapse rate approaches the dry adiabatic limit near z_T since nearly all of the water has condensed and fallen out at lower levels. The temperature lapse rate for subsiding air would follow a dry adiabat in the absence of infrared cooling. The effect of radiative cooling in the region immediately below z_T is to reduce the magnitude of the temperature lapse rate. Parcels of air in a region of subsidence, initially at temperature $T(z_T)$, will tend to be cooler than parcels of cloud air at comparable levels. However, the magnitude of the change in temperature is a function of the time available for radiative cooling. If the air subsides too quickly, radiative processes will be ineffective in cooling air to a temperature less than that within the clouds. Cooling rates decrease with increasing altitude in the upper troposphere. Thus, for higher values of z_T (warmer T_s), the subsidence rate must be smaller to allow sufficient time for radiative cooling to take effect. In addition, at higher T_s, the moist adiabatic lapse rate in the region immediately below z_T no longer approximates a dry adiabat (temperatures at z_T are found to increase with higher surface temperature in spite of the increase in z_T). Thus, the subsiding air must cool by an even greater amount to attain temperatures less than those defined by the moist adiabat. The subsidence rate must be reduced in order to achieve the desired cooling.

These effects combine to impose a limit on the warmest surface temperature that can be accommodated by the model. Figure 6 illustrates the problem for $T_s = 314$K. Clear-sky temperatures are larger than corresponding temperatures along the moist adiabat for altitudes above 10 km. The moist adiabatic lapse rate is approximately 7K km^{-1} in the region just below $z_T = 18$ km. The lapse rate in the clear-sky

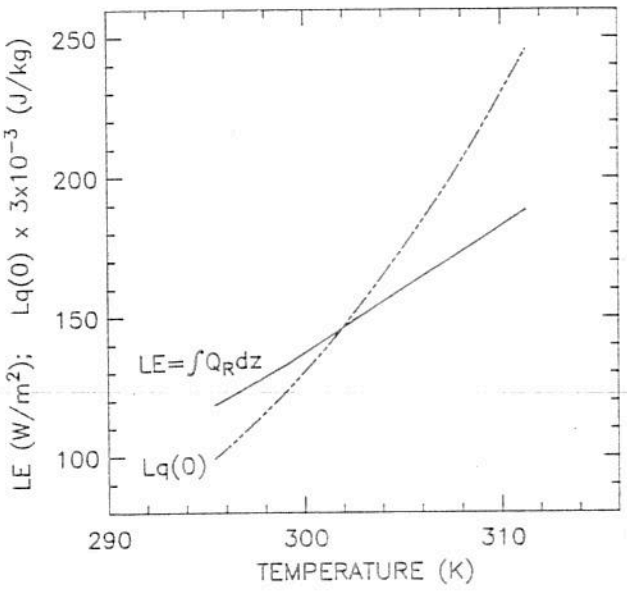

FIG. 5. SURFACE LATENT HEAT FLUX VS SURFACE TEMPERATURE. The figure shows the magnitude of the latent heat flux at the surface, LE, required in the model, compared with the value of the latent energy at the surface, $Lq(0)$, as a function of surface temperature. The value of $Lq(0)$ is multiplied by a factor of 3×10^{-3} for clarity of presentation. Note that $Lq(0)$ increases with temperature more rapidly than LE, so that the ratio $E/q(0)$ is expected to decrease with increasing surface temperature.

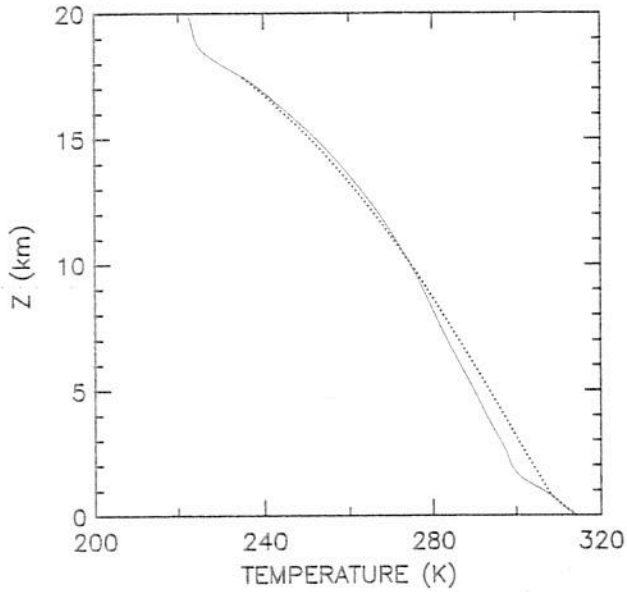

FIG. 6. MODEL TEMPERATURES, $T_s = 314$K. The solid curve refers to clear-air temperatures calculated by the model and the dotted curve represents cloud temperatures. Note the excess buoyancy below 5 km and the region of negative buoyancy above 10 km. The cloud top is at 18 km.

environment is larger than in the region of cumulus updrafts because the mass flux is not small enough to allow radiative cooling to have sufficient impact on the temperature of subsiding parcels. At lower altitudes, where radiative cooling rates are much larger, the mass flux is too small. In this region the model responds by increasing the static stability so that the rate of subsidence heating, $c_p M_c (dT/dz + \Gamma)$, can balance the larger rate of radiative cooling. The result is that the temperature difference between the subsiding air and cloudy air in the 2–5 km region is too large, about 5–8K. Although Fig. 6 does not display virtual temperatures, the buoyancy problem is similarly evident in comparing cloudy and clear-air virtual temperatures. (The virtual temperature is appreciably different from the actual temperature only when the mixing ratio of water is larger than about 1 g kg^{-1}, thus there is practically no difference above 10 km. Below 10 km, consideration of virtual temperatures results in an increase in the contrast of temperature between cloudy and clear air.)

The magnitude of the decrease in M_c as a function of increasing surface temperature depends on the level of CO_2, as indicated in Fig. 4. The mass flux decreases more rapidly with increasing surface temperature for 700 ppm CO_2 compared with the case for 280 ppm CO_2. This behavior is related to the dependence of the integrated rate of radiative cooling on surface temperature. The increase in the magnitude of the integrated rate of radiative cooling with increasing surface temperature is not as great at higher levels of CO_2; increases in cooling rates are moderated as CO_2 bands become optically thick. The amount of water vapor at the surface is independent of CO_2 for our model, depending only on surface values of relative humidity and temperature. According to equation (10), the magnitude of M_c decreases more rapidly with increasing surface temperature for higher levels of CO_2.

3.2. *Dependence of emergent i.r. flux on surface temperature*

Our model includes 40 wavenumber bands to define the spectrum of i.r. emission arising from the surface and atmosphere. The choice of spectral intervals is designed to furnish an adequate simulation of processes affecting the transfer of radiation through the atmosphere. It provides in addition a useful low-resolution reproduction of the spectrum of i.r. radiation in the atmosphere. This is illustrated in Fig. 7 for the spectrum of planetary radiation emitted to space. Major features of the emergent flux for a surface temperature of 298K are readily interpreted by comparing results with curves reflecting emission due to blackbodies at temperatures of 250 and 298K. The figure indicates that emission to space for wavenumbers less than 400 cm^{-1} is characterized by a temperature of about 250K, corresponding to an altitude of about 8 km; the rotation bands of H_2O are the dominant features of the spectrum in this wavenumber range. The 1400–1800 cm^{-1} spectral region contains the 6.3 μm band of H_2O and also reflects the cold temperatures of the upper troposphere. The abundance of water vapor in the middle and upper troposphere is clearly important in regulating the integrated emission of infrared radiation to space. The decrease of flux in the 600–750 cm^{-1} region can be attributed to emission to space in the 15 μm band of CO_2. Associated temperatures in this spectral region reflect conditions in colder regions of the upper stratosphere and mesosphere. The window region between 800 and 1200 cm^{-1} is well described by emission of a blackbody at a temperature approximately equal to that of the surface. The absorption feature between 1000 and 1100 cm^{-1} is associated with emission from the lower stratosphere of radiation in the 9.6 μm band of O_3.

We focus in what follows on the integral properties

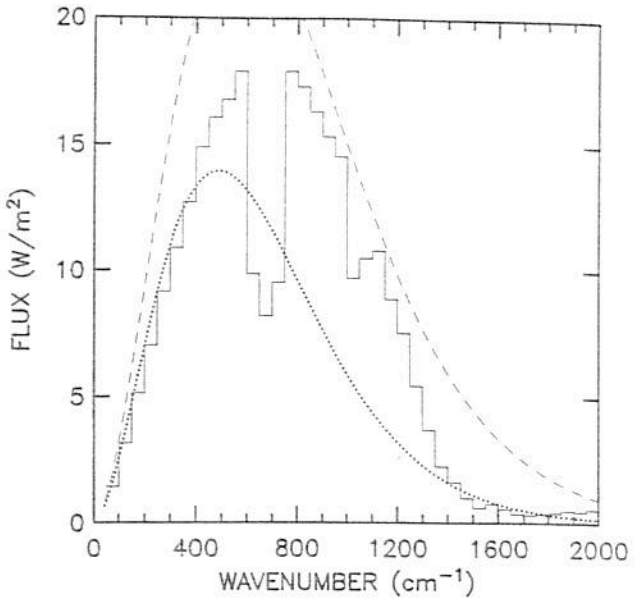

FIG. 7. SPECTRAL DEPENDENCE OF EMERGENT INFRARED FLUX. Calculated values for the emergent infrared flux integrated over 50 cm^{-1} spectral intervals (——) for a surface temperature of 298K are displayed. The abundance of H_2O is consistent with the relative humidity profile used by Manabe and Wetherald (1967); CO_2 is taken at 350 ppm and a climatological mean profile at 10°N is employed for O_3 (Keating and Young, 1985). The radiative flux corresponding to blackbody emission is indicated for temperatures of 298K (– – –) and 250K (·····). Significant features in the emergent flux can be identified at 650 cm^{-1} (15 μm band of CO_2), 1050 cm^{-1} (9.6 μm band of O_3) and 1500 cm^{-1} (6.3 μm band of H_2O).

of the i.r. spectrum, referring to the emergent i.r. flux defined by the area under the histogram in Fig. 7. The dependence of the emergent i.r. flux on surface temperature is summarized in Fig. 8a and b. The sensitivity of the emergent flux to changes in CO_2 is displayed in Fig. 8a. Alternatively, assuming a constant emergent flux, the model provides an indication of the change in surface temperature implied for different levels of CO_2. The results suggest, for an emergent flux of 290 W m^{-2}, that an increase in surface temperature of about 1.4K should ensue for a doubling of CO_2. If instead we were to employ the radiative code using a 6.5K km^{-1} lapse rate adjustment (Manabe and Strickler, 1964), the change in surface temperature would amount to 1.9K. The response of surface temperature to changes in CO_2 in the present model is thus about 25% less for a doubling of CO_2 than that obtained with a convective adjustment model. This decrease in sensitivity was also noted by Lindzen *et al.* (1982) and Lal and Ramanathan (1984), although the reduction obtained in the earlier studies was larger, a consequence, most likely, of the neglect of constraints imposed here by requirements for buoyancy.

The response of the surface temperature to changes in water vapor for 280 ppm CO_2 (Fig. 8b) is about 0.4K per 10% increase in surface relative humidity. The maximum surface temperature allowed by the model is indicated in the appropriate figure. The limit is based on the requirement for positive buoyancy and is determined in general by the rate of radiative cooling near z_T. It is possible to extend the high-T_s limit by increasing the rate for radiative cooling in the upper troposphere relative to that in the lower troposphere. A comparison of model values for the radiative flux with results from the Earth Radiation Budget Experiment (ERBE) provides evidence for moistening of the middle and upper troposphere in excess of that predicted using a fixed profile of relative humidity for surface temperatures greater than about 298K (Minschwaner and McElroy, 1992). Figure 8b summarizes results of calculations which allow for the additional moisture, corresponding to a fixed minimum of 50% in the profile of relative humidity. Moistening of the middle and upper troposphere reduces the dependence of the emergent flux on surface temperature, as expected on the basis of the comparison with ERBE (Minschwaner and McElroy, 1992). For this case, the high-T_s limit is extended to 315K, a result of the increase in cooling rates obtained with higher levels of water vapor in the upper troposphere. The larger cooling rates are responsible in addition for an increase in the height of the cumulus zone z_T (2 km higher for $T_s = 312$K). The dependence of z_T on the

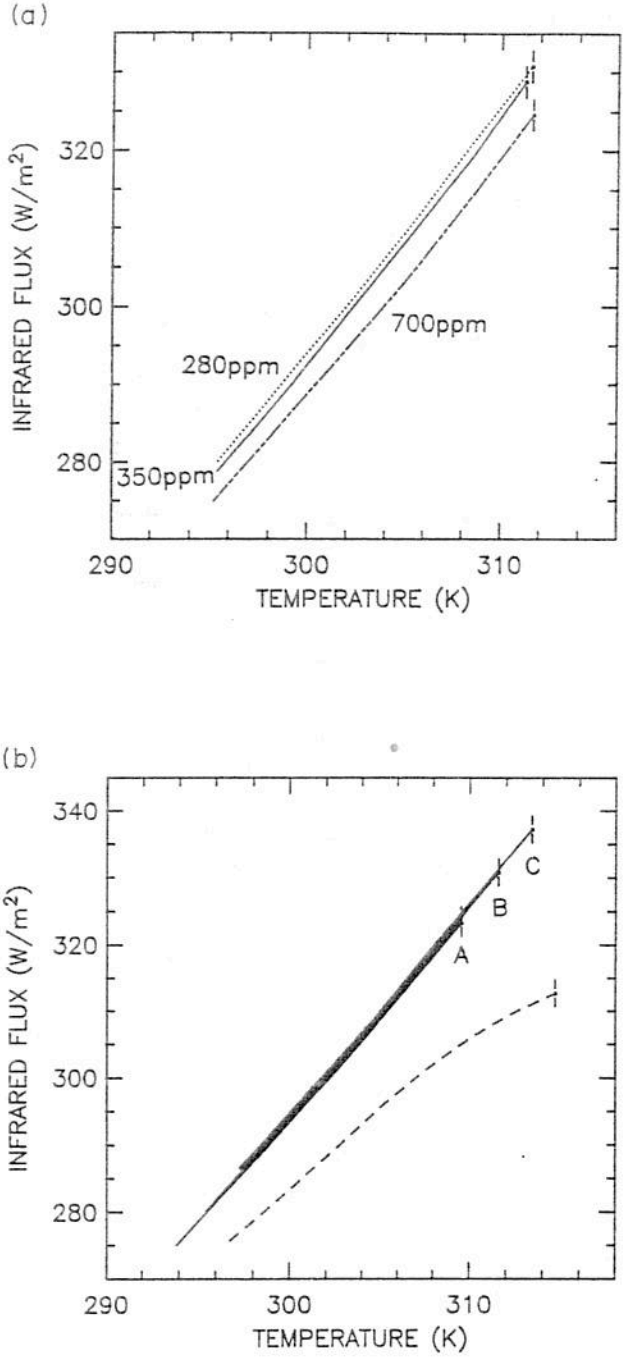

FIG. 8. (a) EMERGENT FLUX VS SURFACE TEMPERATURE, ILLUSTRATING SENSITIVITY TO CO_2.
The figure shows the emergent infrared flux calculated by the model as a function of surface temperature for 280 ppm CO_2(·····), 350 ppm CO_2 (——) and 700 ppm CO_2 (– – –). Short vertical lines indicate the high-temperature limit in each case. (b) Emergent flux vs surface temperature, illustrating sensitivity to surface relative humidity. The emergent infrared fluxes calculated by the model as a function of surface temperature for relative humidities of 70%, 80% and 90% at the surface are indicated by the thick solid line. The short vertical lines denote the high-temperature limit observed for relative humidities of 70% (A), 80% (B) and 90% (C). The dashed curve refers to values of the emergent flux when the model contains additional water vapor in the middle and upper troposphere, corresponding to the assumption of a minimum of 50% in the profile of relative humidity. The level of CO_2 is 280 ppm for all three cases.

magnitude of the emergent flux is indicated in Fig. 9a and b.

3.3. *Sensitivity of β parameter to atmospheric composition*

The upper limit to surface temperatures obtained with the present model precludes the posibility of a runaway greenhouse. The results are consistent in this respect with earlier studies (Lindzen *et al.*, 1982; Lal and Ramanathan, 1984), although the reasons for the conclusion are different. Suppression of a runaway greenhouse effect was attributed in previous work to the ability of the model to deposit increasing fluxes of latent and sensible heat in the upper troposphere. Increases in the temperature of the upper troposphere are more effectively accommodated by enhanced radiation to space, resulting in a reduced efficiency for the greenhouse feedback. However, in earlier studies the limitation imposed by requirements for buoyancy was ignored. We found here that the high-temperature limit was set primarily by the buoyancy constraint. Our results suggest that surface temperatures are restricted to values less than about 312K; for an atmosphere with additional water in the upper troposphere, the limit can be extended to about 315K. The sensitivity of surface temperatures to changes in the solar constant is increased when the upper troposphere contains additional moisture. The sensitivity of surface temperature to changes in the solar constant is defined by a parameter, β, given by (Schneider and Mass, 1975):

$$\beta = S_0 \frac{dT_s}{dS}, \tag{14}$$

where S is the solar constant and $S_0 = 1365$ W m^{-2} denotes the current value of the solar constant. We assumed $F_0 = S_0(1-\alpha)/4 = 259$ W m^{-2}, where $\alpha = 0.24$ is the mean albedo for the tropics (assumed constant), so that:

$$\beta = F_0 \frac{dT_s}{dF}, \tag{15}$$

where F is the magnitude of the emergent i.r. flux as given in Fig. 8a and b; β is a function of T_s, but within the range of T_s shown in Fig. 8a and b, β is nearly constant, equal to 81K for 350 ppm CO_2 and 85K for 700 ppm CO_2. In agreement with Lal and Ramanathan (1984), we obtain larger values for β (about 140K) when the model allows for additional quantities of water vapor in the upper troposphere.

An interesting feature of the present results is the absence of asymptotic behavior in values derived for surface temperature as a function of the solar con-

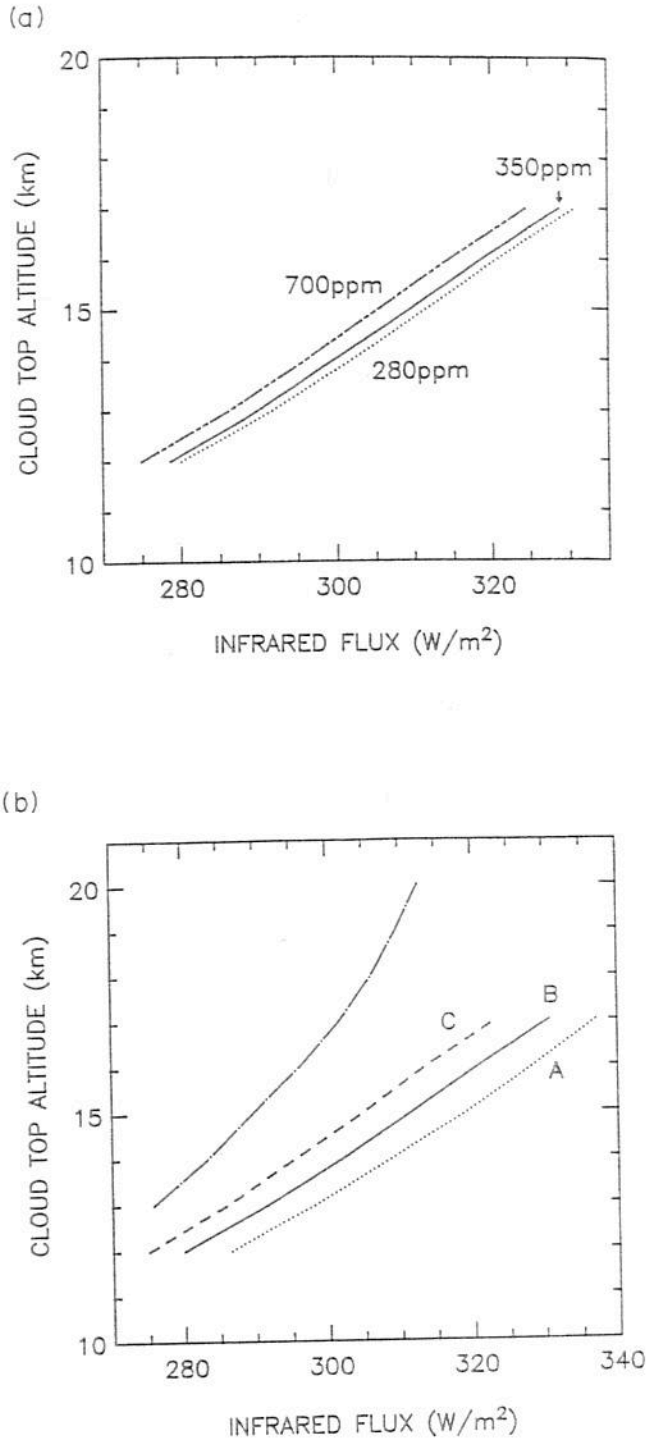

FIG. 9. (a) HEIGHT OF CLOUD TOP VS EMERGENT FLUX, ILLUSTRATING SENSITIVITY TO CO_2.
The figure shows the height of the cloud top, z_T, calculated by the model as a function of the emergent i.r. flux for 280 ppm CO_2 (····), 350 ppm CO_2(——) and 700 ppm CO_2 (– – –). (b) Height of cloud top vs emergent flux, illustrating sensitivity to surface relative humidity. The height of the cloud top, z_T, calculated by the model is shown as a function of surface temperature for surface relative humidities of 70% (*A*, ····), 80% (*B*, ——) and 90% (*C*, – – –). The dot-dash curve refers to values of the emergent flux when the model contains additional water vapor in the middle and upper troposphere, corresponding to a minimum of 50% in the profile of relative humidity.

stant; the magnitude of β remains essentially constant as surface temperature approaches its limiting value. The results suggest that, in addition to the limit $T_s < 312$K, the model is incapable of simulating values of absorbed solar energy greater than about 330 W m^{-2}. If the upper troposphere contains additional moisture, the limit is reduced to about 313 W m^{-2}. Alternative formulations were tested in attempts to extend the model beyond these limits; we considered, for example, the possibility that rising air was saturated with respect to water as it left the surface, and explored also, using a crude simulation, the radiative effect of a 1 km thick cirrus shield immediately below z_T. Neither approach was successful in accommodating higher fluxes of absorbed solar energy. We assumed an emissivity of one, independent of wavelength, in treating the effects of clouds. Effects of clouds on shortwave heating were ignored. It was found that clouds induced a smaller mean-layer cooling rate, in opposition to the behavior required to extend the model to higher surface temperatures [see Slingo and Slingo (1988) for an excellent discussion of the effects of clouds on longwave cooling rates].

It is possible that the limiting behavior found here is an intrinsic consequence of our assumption of a height-independent mass flux. The constant mass flux model is intended to represent the effect of a spectrum of cumulus towers with detrainment levels scattered about a mean level, z_T. One would expect the dispersion of levels to depend critically on the distribution of moist static energy at the surface, as well as on complications introduced by entrainment of environmental air into ascending cumulus towers. We were unable to model either of these effects explicitly using our one-dimensional model, but measurements of the mean subsidence mass flux offer an empirical solution. The observations presented in Fig. 2 indicate that the subsidence mass flux is largest in the 8–10 km region and that it approaches zero at the tropopause (Balsley *et al.*, 1988). Weak subsidence was observed also in the lower stratosphere. We relaxed the constraint of constant mass flux in the model by allowing M_c to decrease linearly with increasing altitude within a 4 km region immediately below the level of the cloud top. Figure 10 indicates that the calculated temperature profile is improved somewhat compared to the case of constant M_c illustrated in Fig. 6. The clear-air temperature profile in Fig. 10 retains, however, a region of negative buoyancy within the 10–14 km altitude range. The region of negative buoyancy corresponds to altitudes where the mass flux was taken as constant (z_T was 19 km in this case; M_c was constant up to 15 km and was assumed to decrease linearly to zero at

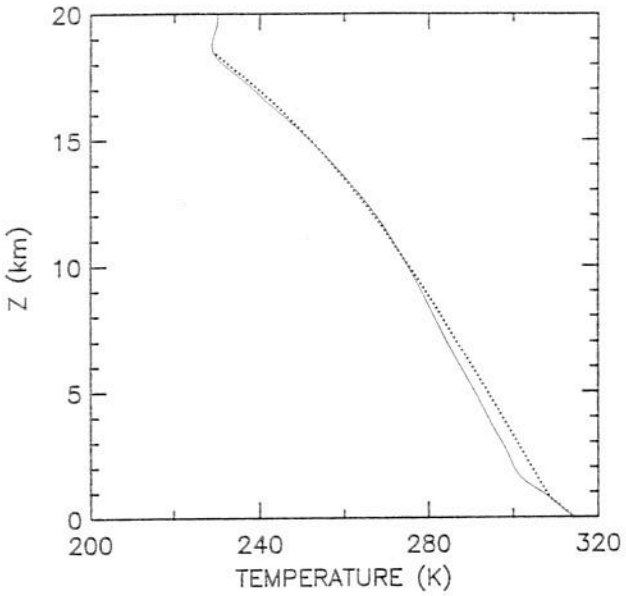

FIG. 10. MODEL TEMPERATURES ILLUSTRATING EFFECTS OF VARIABLE MASS FLUX.
The solid curve refers to clear-air temperatures calculated assuming a constant mass flux from the lifting condensation level (0.52 km) to 15 km. Between 15 km and the cloud top, the mass flux is assumed to decrease linearly with altitude, reaching zero at 20 km.

20 km). This suggests that it may be possible to obtain a satisfactory result by extending the region of variable mass flux to lower altitudes. In the extreme case, this would require large adjustments to the mass flux profile to accommodate specific conditions of temperature and composition. Such a procedure is necessarily *ad hoc* and was judged of limited use for the formulation presented here, particularly so since the profile for H_2O was assumed rather than calculated.

4. CONCLUSIONS

The model presented here is successful in simulating the mean thermal structure of the contemporary tropical atmosphere. The dominant resistance to the tropical circuit described in Section 1 is represented by regions of clear-air descent; the subsidence mass flux is constrained not to exceed a critical limit defined by the net radiative cooling of the troposphere. The cloud detrainment level is raised and the mass flux decreases with increasing surface temperature. A similar pattern was observed by Mitchell and Ingram (1992) in studying the effects of elevated CO_2 using a general circulation model. It is argued here that this behavior is regulated by the competing effects of radiative cooling and subsidence heating in the region of the atmosphere immediately below the mean level for detrainment of the deep cumulonimbus clouds.

The sensitivity of the model to absorbed solar energy and changes in atmospheric composition was examined, predicated on the assumption that the dominant resistance in the tropical circuit was imposed in regions of descent. The relation between the flux of absorbed solar energy and surface temperature, expressed through the β parameter, was found to be relatively insensitive to variations in CO_2 and to uniform changes in the profile of water vapor. The value of β was nearly twice as large for an atmosphere containing additional quantities of water vapor in the middle and upper troposphere, as reflected by results obtained with a model in which the profile for H_2O was constrained to maintain a minimum of 50% in the profile of relative humidity.

The requirement that rising air remain buoyant to z_T implies a limit to the magnitude of the permissible surface temperature and to the flux of absorbed solar energy that can be reconciled with the current mode of circulation for the tropics. It was found that the surface temperature could not exceed 312K, while the permissible range for the flux of absorbed solar energy was restricted to values less than 330 W m^{-2}. These limits were found to depend on the profile for water vapor, but in no case were we able to extend the range of surface temperatures beyond 315K. The limits on surface temperature and permissible flux obtained here may be artificial in the sense that they arise as a consequence of simplifying assumptions concerning the dependence of the subsidence mass flux on altitude. Higher surface temperatures could be realized by relaxing this assumption; this would require, however, large changes with respect to the contemporary atmosphere in the profile for subsidence as a function of altitude.

The results underscore the importance of the interaction between the ocean surface and the atmosphere, beginning with the coupling of the surface temperature field to the temperature and humidity of the mixed layer over the warm pool, continuing through the connection to the upper troposphere through deep convection, culminating in a return to the surface regulated by subsidence and radiative cooling. The extreme sensitivity of the tropical climate to details of the subsidence mass flux implied by the present model suggests that this quantity could provide an important indicator of climate change. Possible trends in quantities linked to M_c, such as surface wind speed, mixed layer relative humidity, and the sea–air temperature difference, deserve closer scrutiny. Variations in these key parameters could provide an important early indicator of possible anthropogenically linked changes in climate.

Acknowledgements—K. Minschwaner gratefully acknowledges fellowship support from the Alexander Host Foundation; additional support was provided by National Science Foundation grant ATM-89-21119 to Harvard University. We thank Brian F. Farrell for a number of useful discussions. This paper is published with appreciation to David Bates for his friendship and counsel and for his generous and unselfish years of public service as Editor-in-Chief of *Planetary and Space Science*.

REFERENCES

Balsley, B. B., Ecklund, W. L., Carter, D. A., Riddle, A. C. and Gage, K. S. (1988) Average vertical motions in the tropical atmosphere observed by a radar wind profiler on Pohnpei (7°N latitude, 157°E longitude). *J. atmos. Sci.* **45**, 396.

Bolton, D. (1980) The computation of equivalent potential temperature. *Mon. Weather Rev.* **108**, 1046.

Ferrier, B. S. and Houze, R. A. (1989) One-dimensional time-dependent modeling of GATE cumulonimbus convection. *J. atmos. Sci.* **46**, 330.

Gray, W. M. (1973) Cumulus convection and larger scale circulations I. Broadscale and mesoscale considerations. *Mon. Weather Rev.* **101**, 839.

Hess, S. L. (1959) *Introduction to Theoretical Meteorology*. Holt, Rinhart and Winston, New York.

Keating, G. M. and Young, D. F. (1985) Interim reference ozone models for the middle atmosphere. In *Handbook for MAP* (Edited by Labitzke, K., Barnett, J. J. and Edwards, B.), Vol. 16, p. 205. SCOSTEP Secretariat, University of Illinois, Urbana, IL.

Lal, M. and Ramanathan, V. (1984) The effects of moist convection and water vapor radiative processes on climate sensitivity. *J. atmos. Sci.* **41**, 2238.

LeMone, M. A. and Zipser, E. J. (1980) Cumulonimbus vertical velocity events in GATE. Part I: diameter, intensity and mass flux. *J. atmos. Sci.* **37**, 2444.

Lindzen, R. S., Hou, A. Y. and Farrell, B. F. (1982) The role of convective model choice in calculating the climatic impact of doubling CO_2. *J. atmos. Sci.* **39**, 1189.

Manabe, S. and Strickler, R. F. (1964) Thermal equilibrium of the atmosphere with a convective adjustment. *J. atmos. Sci.* **21**, 361.

Manabe, S. and Wetherald, R. T. (1967) Thermal equilibrium of the atmosphere with a given distribution of relative humidity. *J. atmos. Sci.* **24**, 241.

McClatchey, R. A., Fenn, R. W., Selby, J. E. A., Volz, F. E. and Garing, J. S. (1972) Optical properties of the atmosphere. Environmental Research Paper 411, U. S. Air Force Cambridge Research Laboratory, Bedford, MA.

Minschwaner, K. and McElroy, M. B. (1992) A model for the energy budget of the atmosphere: comparison with data from the Earth Radiation Budget Experiment. *Planet. Space Sci.* **40**, 1237.

Mitchell, J. F. B. and Ingram, W. J. (1992) Carbon dioxide and climate: mechanisms of changes in cloud. *J. Climate* **5**, 5.

Newell, R. E., Kidson, J. W., Vincent, D. G. and Boer, G. J. (1972) *The General Circulation of the Tropical Atmosphere*, Vol. 1. MIT Press, Cambridge, MA.

Ogura, Y. and Cho, H. (1973) Diagnostic determination of cumulus cloud populations from observed large-scale variables. *J. atmos. Sci.* **30**, 1276.

Oort, A. H. (1971) The observed annual cycle in the meridional transport of atmospheric energy. *J. atmos. Sci.* **28**, 325.

Riehl, H. and Malkus, J. S. (1958) On the heat balance of the equatorial trough zone. *Geophysica* **6**, 503.

Sarachik, E. S. (1978) Tropical sea surface temperature: an interactive one-dimensional atmosphere ocean model. *Dyn. atmos. Oceans* **2**, 455.

Satoh, M. and Hayashi, Y. (1992) Simple cumulus models in one-dimensional radiative convective equilibrium problems. *J. atmos. Sci.* **49**, 1202.

Schneider, E. K. (1977) Axially symmetric steady-state models of the basic state for instability and climate studies. Part II. Nonlinear calculations. *J. atmos. Sci.* **34**, 280.

Schneider, S. H. and Mass, C. (1975) Volcanic dust, sunspots, and temperature trends. *Science* **190**, 741.

Slingo, A. and Slingo, J. M. (1988) The response of a general circulation model to cloud longwave radiative forcing. I: introduction and initial experiments. *Q. J. R. Met. Soc.* **114**, 1027.

Sun, D.-Z. and Lindzen, R. (1992) Negative feedback of water vapor inferred from the mountain snowline record. *Ann. Geophys.* (in press).

Xu, K. and Emanual, K. A. (1989) Is the tropical atmosphere conditionally unstable? *Mon. Weather Rev.* **117**, 1471.

Yanai, M., Esbensen, S. and Chu, J. (1973) Determination of bulk properties of tropical cloud clusters from large-scale heat and moisture budgets. *J. atmos. Sci.* **30**, 611.